Progress In Electromagnetics Research B, Vol. 44, 427–445, 2012

NEW ALGORITHMS FOR THE SPECIFIC ABSORPTION RATE NUMERICAL EVALUATION BASED ON SPHERICAL AVERAGING VOLUMES

L. Catarinucci* **and L. Tarricone**

Department of Innovation Engineering, University of Salento, Via per Monteroni, Lecce 73100, Italy

Abstract—The numerical calculation of the Specific Absorption Rate (SAR) averaged over a certain tissue mass is a common practice when evaluating the potential health risk due to the human exposure to electromagnetic sources. Nevertheless, SAR values are strongly influenced by many factors such as, for instance, the shape of the volume containing the reference mass, the spatial discretization step, or the treatment of internal air, just to mention some of them: different choices can induce significant discrepancies. In this work, an overview on some of the most commonly adopted SAR algorithms is firstly presented, and a discussion on their potential differences reported. Then, based on a spherical volume approach, some new algorithms are proposed. All the algorithms are then used to evaluate the SAR both in artificially generated test cases and in some practical human-antenna interaction problems. The result comparison highlights relevant discrepancies and enforces the necessity of a reasoned standardization of the techniques for the SAR calculation.

1. INTRODUCTION

In recent years, there has been an increasing public concern about the possible risks for human health due to the interaction with electromagnetic (EM) fields. For this reason, the major world public organizations involved in radioprotection issues have established safety guidelines for radiofrequency exposure, as for instance the IEEE RF Safety Standard C.95.1-2006 [1] and the International Commission on Non-Ionizing Radiation Protection (ICNIRP) Safety guidelines [2].

Both documents are based on the specific absorption rate (SAR) averaged over a certain reference tissue mass (rm), which is strongly

Received 15 September 2012, Accepted 10 October 2012, Scheduled 10 October 2012

* Corresponding author: Luca Catarinucci (luca.catarinucci@unisalento.it).

related to the temperature increase caused by the exposure to EM sources. Such averaging mass is usually 1 g, 10 g or the whole body mass. More specifically, apart from some regional lows and the previous IEEE standard [3], which refer to $rm = 1\,\mathrm{g}$, both [1, 2] refer to $rm = 1\,\mathrm{g}$. Safety limits are accurately fixed distinguishing among different categories of workers and different body parts, and they are also frequently updated as a consequence of the results produced by the scientific community. For instance, a confirmation of that is given by the introduction for the first time in a guideline [1] of specific safety limits for the pinna which take into account the anatomic details of the ear and their effects in the exposure to cellular phones [4–6]; such diversification had not been considered neither in the previous IEEE standards [3, 7] nor in ICNIRP guideline.

Nevertheless, in contraposition to the attention dedicated to the refinement of the safety limits, it is quite evident a lack of indications about how the SAR should be evaluated. As well known, in fact, the SAR averaged over a certain reference mass, can be written as:

$$SAR_{rm} = \frac{\int_{V(rm)} \sigma \left|E\right|^2 / 2_d v}{\int_{V(rm)} \rho_d v}, \tag{1}$$

where σ [S/m] is the tissue conductivity, E [V/m] the electric field, ρ [kg/m^3] the tissue density, rm the reference averaging mass and $V(rm)$ is a volume containing rm.

It can be noted that the shape of the volume containing rm does not affect the divisor of (1), which always converges to rm. Vice versa, it does affect the dividend; in fact, the distribution of the electric field varies greatly from point to point inside the tissues, so that the use of different volumes could generate appreciable discrepancies.

It is reasonable wondering, hence, how the shape of the volume containing the reference mass could impact the SAR value itself and if, consequently, such a shape must conveniently be standardized. A spherical volume is the most logical choice, because it naturally selects the points which are as close as possible to the evaluation point. Moreover, it has been demonstrated in [8] that the correlation between averaged SAR and temperature increase is better when spherical instead of cubical averaging volumes are considered. Nonetheless, IEEE standard bases its safety limits on cubical volume, whilst ICNIRP guidelines is referred to SAR values averaged on any 10 g of continuous tissue, but no specific algorithms are suggested.

Moreover, it is worth recalling that, if Finite Difference Time Domain methods or other numerical techniques are adopted to estimate the electric field, a discretized simulation domain is used and the

averaged SAR can be computed through the following formula:

$$SAR_{rm} = \frac{\sum\limits_{i \in \bar{V}(rm)} \left(\sigma_i \left| E_i \right|^2 / 2 \right) \Delta V}{\sum\limits_{i \in \bar{V}(rm)} \rho_i \Delta V}, \tag{2}$$

where the index i indicates the generic elementary cell of the discretized space and $\bar{V}(rm)$ the discretized volume containing the reference mass rm. The use of a certain volume $\bar{V}(rm)$, the adopted spatial discretization step, and other issues, can impact upon the estimation of (2). Indeed, the use of a volume consisting of several cells, is itself a degree of freedom and consequently a source of non-uniqueness of the results, as the SAR value depends on which cells are chosen to better represent the desired volume shape. Moreover, also the spatial discretization step could play a major role: a space step as large as a significant portion of the reference mass, for instance, other than emphasizing the just mentioned problem, causes averages computed over mass values different from the desired rm.

Moreover, it is worth recalling that the peak SAR value is often found in points close to the human surface, where the chosen volume shape must be modified in order to consider only tissue and not air. The choice of the best algorithm in that sense is another open issue, discussed in this work.

More specifically, the paper is structured as follows. In Section 2, some commonly used SAR algorithms will be described, and some new ones proposed by the authors presented and discussed in Section 3. In Section 4, such algorithms are then applied and tested on relevant and complex test cases, and results compared. Conclusions are drawn in Section 5.

2. COMMONLY ADOPTED SAR NUMERICAL ALGORITHMS

As a matter of fact, the number of available algorithms for the numerical evaluation of SAR is quite large [9–17] and in this section, a brief overview on the most commonly adopted ones is presented and commented. One of the usually adopted approaches [11, 12], for instance, computes the SAR_{rm} on a certain point by considering the contributes coming from the cells which belong to a cube centered in that point. The peculiarity of such a strategy, here called Fixed-Cube strategy, is that the size of the cube is calculated in a preprocessing phase on the basis of the used spatial discretization step, the average value of the tissues density, and the desired rm. Once the cube size has

been evaluated, the center of the cube is moved up and down in the discretized target, thus selecting the cells whose contribution is used for the SAR_{rm} evaluation. In Figure 1, a schematic and simplified two-dimensional representation of the Fixed-Cube algorithm is represented. It can be observed that if on the one hand the non-modifiability of the volume shape strongly simplify the algorithm implementation, on the other hand many drawbacks arises. First of all, it is worth highlighting that it is practically impossible to find a cube that selects exactly the number of cells needed to obtain a mass equal to rm. In fact, as the cube should be centered in the evaluation point, only cubes having an odd number of cells as side, can be considered. Consequently, if l is the cube side in cell units (with $l = 1, 3, 5, 7, \ldots$), and N_{CELLS} the total number of cells of the cube ($N_{CELLS} = l^3 = 1, 27, 125, 343, \ldots$), it is clear that is quite improbable to find a cube which selects a mass as large as rm. For instance, in the hypothetical case where each cell has a mass of 125 mg, 8 cells are needed to obtain $rm = 1$ g, but no cubes with an odd number of cells as side involves 8 cells. The choice must be done between $l = 1$ and $l = 3$, corresponding to $N_{CELLS} = 1$ and $N_{CELLS} = 27$ respectively. In the first case, the actual averaging mass would be underestimated (125 mg instead of 1 g), in the second case strongly overestimated (3.3 g instead of 1 g). Moreover, when the fixed cube is used to select the SAR contribution in points close to the external surface, cells of air are also selected, thus modifying the averaging mass. In order to avoid the evaluation of the SAR in cases where a too large portion of the volume does not contain tissues, a maximum tolerable percentage of air is imposed: if the percentage of air is superior to the fixed limit, SAR remains undetermined. It is important to observe that such an approach does not allow the evaluation of the absorbed energy in the most external points of the exposed target where, though, high SAR values or even the peak SAR itself, are located.

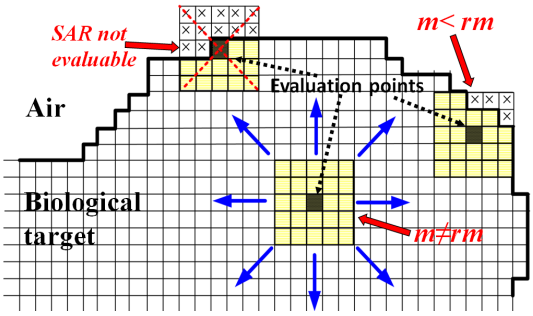

Figure 1. Two-dimensional representation of fixed-cube algorithm.

In [13], a first improvement of the previous technique is obtained through the use of a particular cubical volume which dynamically adjusts its size in order to consider exactly the desired value of rm. The algorithm is here called Fixed Adjustable Cube and it is represented in Figure 2. More specifically, for each evaluation point, the algorithm builds a sequence of cubes of dimension progressively increasing till a mass superior to rm is reached. At each step the percentage of air is evaluated and if it is greater than a prefixed limit, the SAR in that point remains undetermined. Vice versa, the last cube of the sequence with mass inferior than rm is used as the core for the SAR evaluation and only an accurately evaluated portion of the adjacent cells (peripheral cells of the cube) is added in order to exactly reach rm. More specifically, the contribution to the SAR evaluation of the peripheral cells is proportional to the portion of their mass useful to reach rm. Anyhow, a big limit of this algorithm still remains: the incapability to determine the SAR in points closed to the surface of the exposed target.

In [14], a further improvement in that sense is proposed; the concept of a volume perfectly cubical is not considered indispensable anymore; the cells are assembled around the reference point one by one following established criteria and excluding air. The algorithm, here named Adaptive Cube (AC) and represented in Figure 3, stops the insertion of new cells when the total mass is equal to rm. Note that the resultant averaging volume is given by the set of cells belonging to the intersection between a cube and the non-tissue points. In such a way, the SAR can be evaluated in every point, including those belonging to the most external biological target.

Another alternative algorithm is that reported in [15]. It is here called C95.3 and a two-dimensional representation is reported

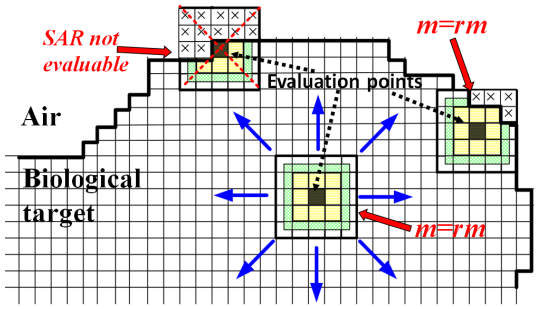

Figure 2. Two-dimensional representation of fixed adjustable cube algorithm.

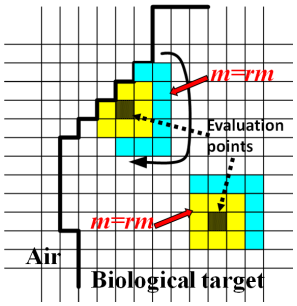

Figure 3. Two-dimensional representation of adaptive cube algorithm.

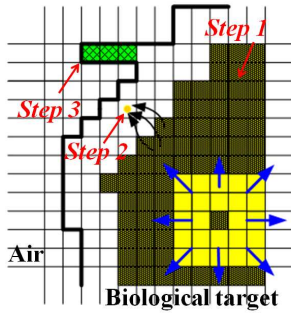

Figure 4. Two-dimensional representation of C95.3 algorithm.

in Figure 4; though recommended in [1], it has some drawbacks. In C95.3, three different phases are necessary. In the first one, the SAR_{rm} is evaluated, wherever possible, by using a fixed-cube strategy with the tolerable air percentage set to zero and only if rm is reached with tolerance of 5%. It is worth highlighting that the fulfilment of such a requirement strongly depends on the discretization step, other than the tissue density ρ of each involved cell, so that in some cases SAR cannot be evaluated unless such requirement is ignored. In the second phase, the SAR in each one of the undetermined points is imposed as the maximum of the already evaluated SAR among those whose cube contained that point. Finally a third phase is applied in the remaining points (usually belonging to extremities): the point becomes the center of a face of a new cube which can contain air and is extended till a mass of rm is selected. This algorithms allows the evaluation of the SAR in every point. Nevertheless, the second phase of the algorithm, referred to the very critical points close to the target surface, assigns to such points SAR values referred to more internal points, thus causing a possible underestimation of the peak SAR, as will be discussed in Section 4.

The comparison among the presented numerical techniques shows that even radically different algorithms for the evaluation of the SAR can comply with the few indications reported in RF safety guidelines, despite it is easily predictable that they could generate discrepant results. Moreover, all of them are based on a cubical volume shape, which on the one hand allows an easy implementation, but on the other hand it does not seem to be the most logical choice because it does not select the most close cells to the evaluation point.

In the next section, some new algorithms based on spherical integration volumes are proposed and discussed.

3. NEW SAR ALGORITHMS BASED ON SPHERICAL AVERAGING VOLUMES

According to the previous discussion, the first point to be clarified is about the shape of the integration volume. A spherical volume is the ideal choice. Spheres, in fact, select the nearest cells to a reference point, thus allowing the most natural evaluation of the SAR Nevertheless, to adequately take into account a spherical volume when discretized spaces are considered, some observations are necessary. In the continuous space, in fact, it is possible to determine a sphere (a circle in 2D) which exactly contains a quantity of tissue equal to rm. Such a sphere becomes a so-called ideal sphere when it is evaluated in the discretized space. For the 2D case, an hypothetical ideal circle is reported in Figure 1; the cell in the center (in yellow) represents the point where the SAR must be evaluated. With respect to the ideal circle, three different classes of cells can be individuated: internal, external and peripheral cells. The internal cells are those which are completely enclosed in the ideal circle (yellow, light blue and green in Figure 5), so that they are fully taken into account in the evaluation of the SAR. Vice versa, the external cells are completely outside the circle, so that they do not give any contribution to the SAR. The cells classified as peripheral are intersected by the ideal circle (the violet ones) and will play a major role in the formulation of new algorithms. The SAR, in fact, should ideally be calculated by adding the contributions of the internal cells to those of every peripheral cell, accurately weighted on the bases of its actual internal mass. The different strategies used for the evaluation of the partial volume/mass to be considered for each one of the peripheral cells, characterize the new algorithms presented in the following sub-sections.

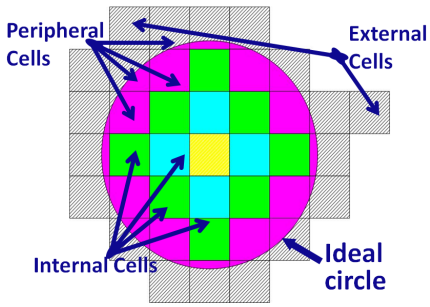

Figure 5. Representation of the ideal circle in the discretized space. The contribution of peripheral cells to the SAR value must be accurately weighted on the bases of the portion of internal mass/volume.

3.1. Onion Skin Algorithm

The first spherical algorithm which is here proposed considers a sphere as the reference volume and, when necessary, modifies the shape in order to include only tissues and not air. Starting from the evaluation point as initial partial volume, the mass is evaluated and new cells are added to the partial volume one by one so as to reach the desired rm. The strategy that regulates the addition of a new cell to the partial volume, gives the name to the proposed algorithm, shown in Figure 6, and called "Onion Skin" (OS); if the mass contained in a sphere of radius r (onion) is inferior to rm, in fact, new cells are added selecting them out among those belonging to the layer which radius is $r + 1$ (skin). Such an algorithm is similar to the AC one proposed in [14] apart from the shape of the volume.

The main steps of the algorithm for the evaluation of the SAR_{rm} in a cell of coordinates $\langle x, y, z\rangle$ can be synthesized as follows:

1. initialize the radius $r = 1$ and set the center in $\langle x, y, z\rangle$;
2. select the set of possible candidate cells as those belonging to the layer of radius r centered in $\langle x, y, z\rangle$ and representative of tissues (air is excluded);
3. add one of the individuated cell to the partial volume and compute the new partial mass pm.
4. repeat step 3 until all the cells individuated in 2 have been added or the condition $pm \geq rm$ is verified;
5. if $pm \geq rm$ has not been verified yet, impose $r = r + 1$ and come back to 2. Else (the volume is founded) go to 6;
6. Evaluate the SAR_{rm} by using the individuated volume.

The method guarantees that the desired 1 g or 10 g of rm are obtained with a tolerance on the order of a fraction of the last added cell mass and allows the SAR evaluation in each tissue point. Nevertheless,

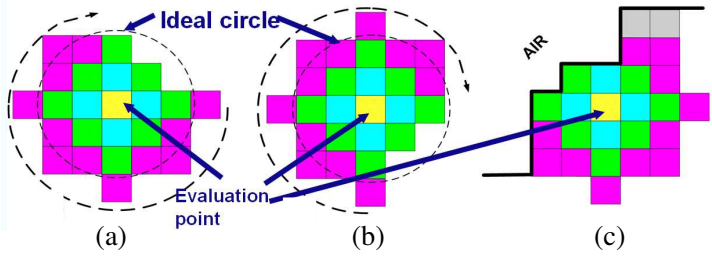

Figure 6. Onion skin algorithm applications examples.

some minor drawbacks do exist: the non-uniqueness in the choice of the peripheral cells to be considered in the computation, and the possible unbalancing of the resultant volume with respect to the evaluation point. In fact, as said, the algorithm ends the insertion of new cells as soon as rm is reached, so that the last skin of the sphere, which is in most cases uncompleted, is composed of a certain number of cells chosen among all the peripheral ones. Consequently, there are different valid peripheral cells combinations depending on the insertion strategy adopted in the step 3 of the algorithm, so that the SAR uniqueness is not guaranteed.

For instance, in Figures 6(a) and 6(b), a two-dimensional schematization of the volume individuated by the OS algorithm is reported for a simple case of absence of air and supposing that 25 cells guarantee a mass of almost rm. More specifically, the evaluation point is supposed to be far enough from every air region so that for each successive layer all the cells can be considered potential candidates to be part of the averaging volume; as apparent, three complete layers and a partial one are needed. However, the cells of the last layer, i.e., the peripheral cells, could be chosen in different ways as evident by comparing Figure 6(a) and Figure 6(b), and consequently the obtained SAR could assume different values. This represents the most substantial lack of the OS algorithm, and it is substantially due to the approximation introduced in the evaluation of the portion of peripheral cells to be considered for the SAR evaluation in spherical algorithms. In the OS algorithm, instead of evaluating the portion of every single peripheral cell internal to the ideal circle, the contribution to the SAR value of some of the peripheral cells is entirely considered, whilst the contribution of some others is not considered at all.

Finally, Figure 6(c) shows what happens when the evaluation cell is quite close to air regions, with the consequent modification of the volume shape in order to guarantee anyhow an averaging mass equal to rm as well as the use of only tissue cells.

3.2. Graded Peripheral Cell Algorithm

As previously observed, the best way for considering spherical volumes in orthogonal meshes, would be that of taking into account the whole contribute coming from all the cells entirely contained in the ideal sphere, and the partial contribute given by the peripheral cells. The problem, actually not trivial, consists on the accurate evaluation of the partial volume to be considered for each of the peripheral cells; this problem is quite difficult to solve analytically because of the high number of possible intersections between spheres and cubes: approximations are, hence, strongly necessary.

Differently from OS, the herein proposed approach, called Graded Peripheral Cells (GPC), takes into account the contribution of all the peripheral cells. More specifically, an equal fraction of all the peripheral cells, regardless to the effective volume individuated by the ideal sphere (or ideal circle in 2D), is considered. The algorithm analyzes all the non-air cells around the evaluation point, and marks them as internal, external or peripheral, respect to the ideal sphere (in order to perform such an operation, the number of vertexes internal to the sphere is computed).

Once such an analysis has been performed, the total mass of the internal cells is known, and consequently the portion of mass to be considered among all the peripheral cells in order to reach rm is easily computed. Such a quantity is considered as equally distributed among all the peripheral cells which proportionally will contribute to the final SAR value.

In Figure 7, the individuated resultant volume is reported for the same case of Figure 6(a). The small internal squares sketched inside the peripheral cells, represent the considered portion of mass. By comparing such a volume with the one obtained with the OS algorithm, it can be noticed that the problems of the unbalancing with respect to the central cell and the non-uniqueness of the SAR value, are substantially bypassed. Nevertheless, the assumption that all the peripheral cells contribute with the same mass, seems to be too approximate. Indeed, some of the cells are only slightly intersected from the ideal sphere, and their weight in the SAR computation is the same of some other peripheral cells which are almost completely internal (see Figure 7). The next proposed algorithms can be considered as a further refinement of the GPC one, aimed at better approximate the ideal situation described in Figure 5.

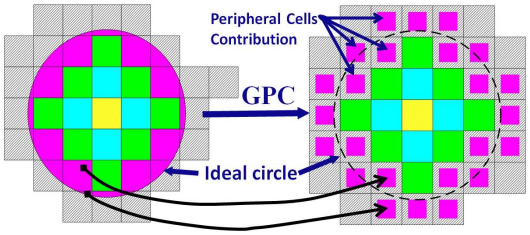

Figure 7. GPC algorithm applications example.

3.3. Graded Peripheral Vertex and Vertex-3 Algorithms

The Graded Peripheral Vertex (GPV) algorithm represents a more refined version of the GPC algorithm. As previously shown, in fact, in GPC the same portion of mass is considered for each one of the peripheral cells; if a method is found for discriminate how much of a cell is internal to the ideal sphere, a non-uniform weighting can be effectively applied. Actually, a cell is peripheral if at least one of its vertexes is internal to the ideal sphere and, at the same time, at least one vertex is external. The number of internal vertexes, hence, could be a good parameter to be used. Despite it is still an approximation, it can be considered that a cell with only one internal vertex contributes with a portion of its volume larger than that of a cell with a greater number of internal vertexes.

The GPV algorithm, hence, calculates the portion of a peripheral cell to be considered, proportionally to the number of internal vertexes; more specifically, if $1 \leq n < 8$ ($1 \leq n < 4$ in 2D cases) is the number of internal vertexes of one of the examined cells, then a portion proportional to $n/8$ of its mass is considered.

Figure 8 shows (reporting also the number of internal vertexes for each peripheral cell) how the application of the GPV algorithm allows a better distribution of the mass respect to the GPC and the OS ones, increasing the accuracy of the approximation with respect to the ideal case of Figure 5 and thus improving the quality of the result.

A slight modification of the GPV algorithm, is the Graded Peripheral Vertex-3 (GPV3) algorithm, where the contribute of each peripheral cell is proportional not to the number of internal vertexes n, but to its cube (its square in 2D), i.e., to n^3. This criterion is based on the observation that the dependence of the internal volume on the number of internal vertexes is, in most cases but not always, almost cubical. In such an algorithm, hence, the mass of a cell is divided into 64 parts (16 in 2D) and $n^3/64$ is the fraction of mass (and volume) considered for a peripheral cell with n internal vertexes.

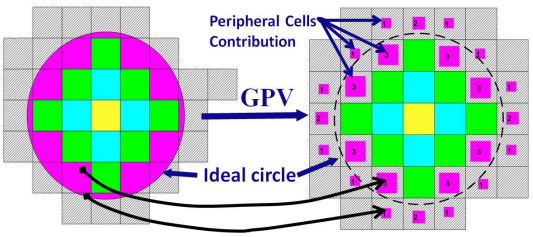

Figure 8. GPV algorithm applications example.

Both GPV and GPV3 guarantee an averaging mass substantially equal to rm and a good estimation of the peripheral cell contributions to the SAR.

4. RESULTS

In this section, some of the presented algorithms are tested on appositely generated test-cases and on the practical problem of the evaluation of SAR in humans exposed to an EM source, and results compared and discussed. More specifically in the first part of this section two homogeneous cubes (named type I and type II respectively) both with side $l = 15\,\text{cm}$ $\sigma = 0.75\,\text{S/m}$ $\rho = 1.015\,\text{g/cm}^3$ and the electric field linearly varying along a direction orthogonal to one face from a maximum of 160 V/m to a minimum of 1 V/m, have been considered: the type I cube is oriented accordingly to a Cartesian reference system, whilst the type II cube is obtained by a 45°-rotation with respect to one axis. Many discretized versions of the cubes have been produced by varying the discretization step from 1 mm to 6 mm, so that the sensitivity of the different algorithms to the discretization step and to the reference system has been investigated.

Results in Figure 9(a), for instance, are referred to the maximum SAR averaged over a mass of 1 g for the type I cube, obtained by using six different algorithms: the C95.3 and the AC, representative of the cubical shape algorithms, the OS one, which applies the same strategies of the AC but to spherical volumes, and the three successive refinements, respectively GPC, GPV and GPV3. Moreover, eleven different discretization steps have been considered. In Figure 9(b), instead, the same kind of data is reported for the type II cube. Note that, as the peak SAR is searched, Fixed-Cube and Fixed Adjustable Cube have not been tested, because they are not able to calculate the SAR in points close to the external surface, as discussed in Section 2.

The first relevant aspect that can be pointed out is the unpredictable, but not surprising, behaviour of the C95.3 algorithm; the first reason is that such an algorithm is in part based on a fixed-cube strategy so that, depending on the discretization step, the averaging mass can strongly differ from rm; for instance, only for the smallest discretization step (1 mm) the percentage difference between actual mass and rm was inferior to 5%, which is the maximum tolerable on [15]. This means that for other discretization steps the algorithm could not be applied. Moreover, C95.3 algorithm tends to underestimate the peak values, because of the saturation effect associated to the phase 2 of the algorithm commented on Section 2. Another important aspect deducible from Figure 9, is the good

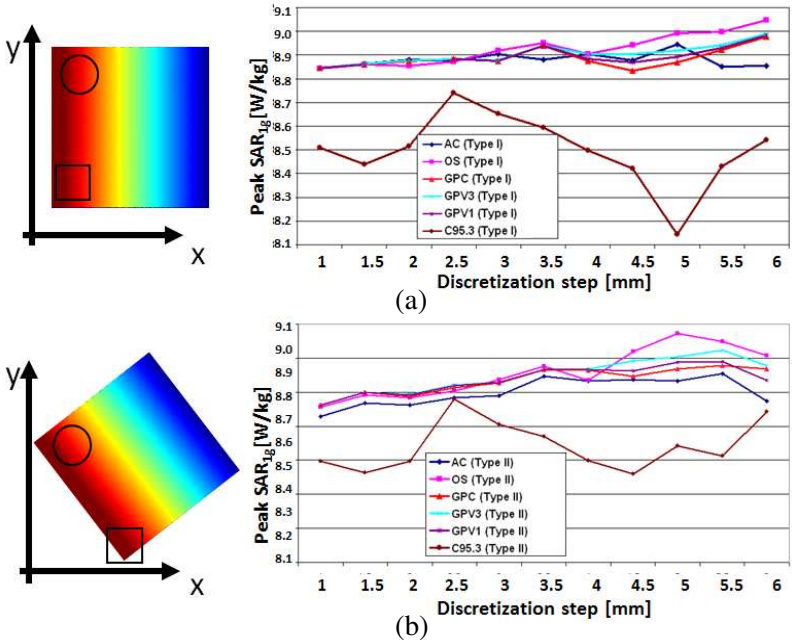

Figure 9. Peak SAR ($rm = 1\,\mathrm{g}$) in an artificially generated cube evaluated through AC, OS, C95.3, GPC, GPV and GPV3 algorithms. The Electric Field varies linearly from 160 V/m to 1 V/m. The discretization step from 1 mm to 6 mm. The type I cube (a) is oriented accordingly to a Cartesian reference system, whilst the type II cube (b) is obtained by a 45°-rotation with respect to one axis.

agreement among GPC, GPV and GPV3, which are the most refined algorithms, and the stronger dependence on the discretization step of AC and OS. Finally, by comparing Figure 9(a) with Figure 9(b), the better attitude of spherical algorithms to deal with the problem is highlighted by the higher discrepancy among results obtained with cubical algorithms (C95.3 and AC on the type I cube versus the same algorithms on the type II) with respect to those obtained with spherical ones.

In order to compare the algorithms on a practical case, the difficult problem of the interaction of a human with the field emitted by a radiobase station antenna has been then solved by using the parallel FDTD method proposed in [18–21] and refined in [22, 23], and the SAR averaged over 1 g and over 10 g of tissue has been evaluated in each point of the head of the exposed subject (which is the numerical phantom proposed in [24] having a discretization step of 4 mm in each

Table 1. Peak SAR values computed through different algorithms.

SAR Algorithm		
SAR Algorithm	Peak SAR (1 g) [W/kg]	Peak SAR (10 g) [W/kg]
Adaptive Cube (AC)	27.93	14.39
Onion Skin (OS)	27.00	14.32
Graded Peripheral Cell (GPC)	27.65	14.73
Graded Peripheral Vertex (GPV)	27.89	14.78
Graded Peripheral Vertex-3 (GPV3)	28.03	14.85
C95.3	25.12	11.05

direction). In Figure 10(a), the electric field distribution in a section of the head is reported. The same six algorithms (C95.3, AC, OS, GPC, GPV and GPV3) have been used. Also in this case the other presented commonly adopted algorithms have not been tested. In fact, their inability to evaluate the SAR in superficial points makes impossible the comparison with the other more sophisticated strategies.

In Table 1, the peak SAR values are reported both for $rm = 1\,\mathrm{g}$ and for $rm = 10\,\mathrm{g}$. It can be observed that, apart from C95.3, all the tested algorithms give comparable results. This is not surprising at all: even if the algorithms are quite different, in fact, the peak SAR is found in the proximity of the phantom surface where the electric field assumes the highest values all around a region as large as many rm. In such points, the volumes are also strongly deformed by the phantom shape, so that the refinement strategies give unappreciable benefit. Anyhow, it is important to recall again that, among the possible, only algorithms which can evaluate the SAR everywhere in the phantom have been tested; the others algorithms, such as the one proposed in [15, 16] or the one proposed in [17], would have been unable to determine the SAR in such points. As for the C95.3 algorithm, also in this case it is apparent that it underestimates the peak value, and this enforces a more detailed discussion, as it is the only algorithm officially suggested in a radioprotection standard.

Because of the peculiarity of the peak SAR, though, results are comparable and the differences among the various algorithms cannot be appreciated. Consequently, a more deep analysis based on all the SAR values, and not only on the peak ones, should be carried out.

In Figure 10(b), for instance, the percentage difference computed point by point between AC and OS is graphically represented. The chromatic scale, from blue to red, represents increasing differences from 0 up to 50%. It is quite apparent the strong diversity in

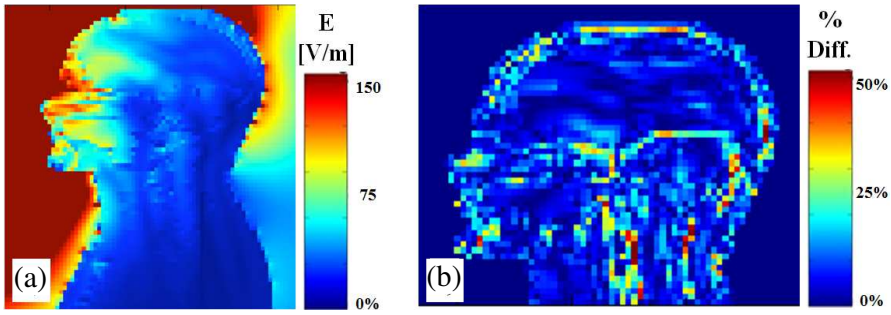

Figure 10. (a) Electric field in the head of a numerical phantom exposed to 900 MHz radiobase antenna and (b) percentage difference between the SAR values evaluated through AC and OS algorithms.

Table 2. Average and maximum percentage difference between GPV3 and the other algorithms.

Percentage Difference				
SAR Algorithm	SAR (1 g)		SAR (10 g)	
	Average %	Maximum %	Average %	Maximum %
AC Vs GPV3	8.43	99.08	5.12	69.95
OS Vs GPV3	6.90	95.39	3.31	53.71
GPC Vs GPV3	4.93	90.14	0.14	3.04
GPV Vs GPV3	2.66	42.89	0.08	2.33

some investigated phantom points, even though only the shape of the integration volume, and not the strategy, differentiates the algorithms.

In Table 2, instead, the GPV3 algorithm is used as the reference one, and the percentage difference with the others is reported. More specifically, SAR has been evaluated with the two algorithms, results have been compared point by point and two parameters have been computed: the average percentage difference and the maximum percentage difference.

Through the analysis of the data reported in the table, some conclusions can be drawn. First of all, by improving the complexity of the algorithms, all the percentages decrease. As expected, hence, by using more refined spherical algorithms a better discrimination of the absorbed power in the various points can be performed, so that the SAR values can be better estimated. Also, it can be observed that differences referred to the $SAR_{10\,g}$ are always inferior to those referred to the $SAR_{1\,g}$ and this for two different reasons: first of all, by increasing rm, the consequent smoothing effect due to the integration

over a bigger volume causes the attenuation of the differences among the methods. Secondly, the number of peripheral cells increases with the volume and the contribute of each of them becomes less relevant.

Even more interesting are the deductions coming from the analysis of the maximum percentage error; for instance, two sophisticated algorithms, such as OS and GPV3, give in some points difference up to 90% for the $SAR_{1\,\mathrm{g}}$ and up to 50% for the $SAR_{10\,\mathrm{g}}$. In order to better appreciate in graphical way such discrepancies, the percentage difference of GPV3 with respect to both OS and GPC for the $SAR_{1\,\mathrm{g}}$ are reported in Figures 11(a) and 11(b).

Once the algorithms have been tested, it becomes useful to investigate their computational complexity, in order to select the algorithm to be used on the basis of a trade-off between computational time and required accuracy. The parameters which mostly impact upon the simulation time are the discretization step, the value of the reference mass and the size of the computation domain. In fact, the finer is the discretization step, the higher is the number of cells necessary to reach rm and to be considered in the SAR computation. Similar considerations can be done also for the value of rm. Finally, the size of the computation domain is proportional to the number of points where SAR should be evaluated.

In Table 3, the CPU time for most of the described SAR algorithms is reported for two different test cases with discretization step of 4 mm, $rm = 1\,\mathrm{g}$, and a number of cells of 10^3 and 60^3 respectively. Tests have been conducted on a standard desktop computer (an Intel Celeron Dual Core G 540, 2.5 GHz, with 4 GB of RAM). As apparent, the computational time increases with the algorithm complexity, and this suggests the use of the faster algorithms in the whole simulation domain and a refinement through a more sophisticated strategy only in some particularly interesting confined regions.

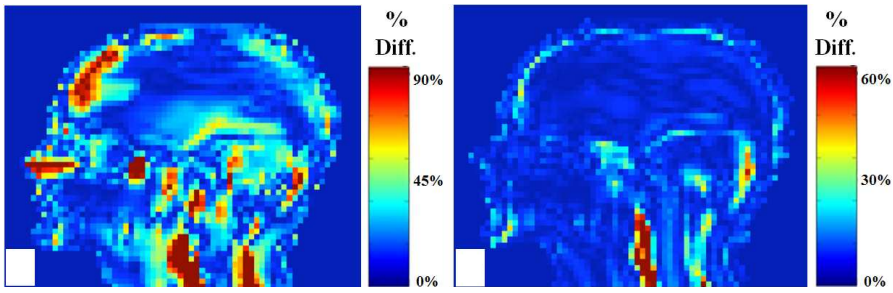

Figure 11. Percentage difference (a) between GPV3 and OS and (b) between GPV3 and GPC for the $SAR_{1\,\mathrm{g}}$.

Table 3. CPU time for the studied algorithms in two different case studies.

SAR Algorithm	CPU time (s): 10^3 Cells Case	CPU time (s): 60^3 Cells Case
C95.3	4"	10"
AC	1"	7"
OS	1"	6"
GPC	5"	6'49"
GPV	10"	12'04"
GPV3	12"	11'45"

5. CONCLUSIONS

In this work, some commonly adopted algorithms for the numerical evaluation of the Specific Absorption Rate (SAR) averaged over a certain mass have been reported and some new ones have been presented and compared. Discrepancies among results obtained through different algorithms are relevant, thus enforcing a more detailed discussion of local SAR values, herein performed, along with an analysis of the shape of the integration volume, the importance of spherical geometries (instead of cubic ones) and other related issues. The four brand new algorithms are suitable alternatives to solve the mentioned problems.

REFERENCES

1. IEEE C95.1-2006, "Standard for safety levels with respect to human exposure to radiofrequency electromagnetic fields, 3 kHz to 300 GHz," IEEE Standards C95.1, Coordinating Committee 28.4, 2006.
2. ICNIRP, "Guidelines for limiting exposure to time-varying electric, magnetic and electromagnetic fields (up to 300 GHz)," *Health Phys.: Intern. Comm. on Non-ionizing Radiation Protection (ICNIRP)*, Vol. 74, 494–522, 1998.
3. IEEE C95.1-1999, "IEEE standard for safety levels with respect to human exposure to radiofrequency electromagnetic fields, 3 kHz to 300 GHz," IEEE Standard C95.1, 1999.
4. Gandhi, O. P. and G. Kang, "Inaccuracies of a plastic "pinna" SAM for SAR testing of cellular telephones against IEEE and ICNIRP safety guidelines," *IEEE Transactions on Microwave Theory and Techniques*, Vol. 52, No. 8, 2004–2012, 2004.

5. Beard, B. B., W. Kainz, T. Onishi, T. Iyama, S. Watanabe, O. Fujiwara, J. Wang, G. Bit-Babik, A. Faraone, J. Wiart, A. Christ, N. Kuster, A.-K. Lee, H. Kroeze, M. Siegbahn, J. Keshvari, H. Abrishamkar, W. Simon, D. Manteuffel, and N. Nikoloski, "Comparisons of computed mobile phone induced SAR in the SAM phantom to that in anatomically correct models of the human head," *IEEE Transactions on Electromagnetic Compatibility*, Vol. 48, No. 2, 397–407, 2006.
6. Burkhardt, M. and N. Kuster, "Appropriate modeling of the ear for compliance testing of handheld MTE with SAR safety limits at 900/1800 MHz," *IEEE Transaction on Microwave Theory and Techniques*, Vol. 48, No. 11, Part 1, 1927–1934, 2000.
7. ANSI C95.1-1982, "American national standard safety levels with respect to human exposure to radiofrequency electromagnetic fields, 300 kHz to 100 GHz," The Institute of Electrical and Electronics Engineers, Inc., New York, NY, 1982.
8. Hirata, A., M. Fujimoto, T. Asano, J. Wang, O. Fujiwara, and T. Shiozawa, "Correlation between maximum temperature increase and peak SAR with different average schemes and masses," *IEEE Transactions on Electromagnetic Compatibility*, Vol. 48, No. 3, 569–577, 2006.
9. Laakso, I., T. Uusitupa, and S. Ilvonen, "Comparison of SAR calculation algorithms for the finite-difference time-domain method," *Phys. Med. Biol.*, Vol. 55, No. 421, 2010.
10. Catarinucci, L. and L. Tarricone, "Specific absorption rate (SAR) numerical evaluation: A critical discussion," *IEEE MTT-S International Microwave Symposium Digest, IMS 2007*, 1349–135, Honolulu, HI, 2007.
11. Nikita, K. S., et al., "A study of uncertainties in modeling antenna performance and power absorption in the head of a cellular phone user," *IEEE Transaction on Microwave Theory and Techniques*, Vol. 48, No. 12, 2676–2685, 2000.
12. Wang, J., O. Fujiwara, S. Watanabe, and Y. Yamanaka, "Computation with a parallel FDTD system of human-body effect on electromagnetic absorption for portable telephones," *IEEE Transactions on Microwave Theory and Techniques*, Vol. 52, No. 1, 53–58, 2004.
13. Caputa, K., M. Okoniewski, and M. A. Stuchly, "An algorithm for computations of the power deposition in human tissue," *IEEE Antennas and Propagation Magazine*, Vol. 41, 102–107, Aug. 1999.
14. Lee, A. and J. Pack, "Study of the tissue volume for spatial-peak mass-averaged SAR evaluation," *IEEE Transactions on EMC*,

Vol. 44, No. 2, May 2002.

15. IEEE C95.3-2002, "IEEE recommended practice for measurements and computations of radio frequency electromagnetic fields with respect to human exposure to such fields, 100 kHz–300 GHz," IEEE Standards C95.3, 2002.
16. Otin, R. and H. Gromat, "Specific absorption rate computations with a nodal-based finite element formulation," *Progress In Electromagnetics Research*, Vol. 128, 399–418, 2012.
17. Wang, M., L. Lin, J. Chen, D. Jackson, W. Kainz, Y. Qi, and P. Jarmuszewski, "Evaluation and optimization of the specific absorption rate for multiantenna systems," *IEEE Transactions on Electromagnetic Compatibility*, Vol. 53, No. 3, 628–637, Aug. 2011.
18. Catarinucci, L., P. Palazzari, and L. Tarricone, "Parallel FDTD simulation of radiobase antennae," *Radiation Protection Dosimetry*, Vol. 97, No. 4, 409–413, 2001.
19. Catarinucci, L., P. Palazzari, and L. Tarricone, "A parallel FDTD tool for the solution of large dosimetric problems: An application to the interaction between humans and radiobase antennas," *IEEE MTT-S International Microwave Symposium Digest*, Vol. 3, 1755–1758, 2002.
20. Catarinucci, L., P. Palazzari, and L. Tarricone, "Human exposure to the near field of radiobase antennas — A full-wave solution using parallel FDTD," *IEEE Transactions on Microwave Theory and Techniques*, Vol. 51, No. 3, 935–940, 2003.
21. Catarinucci, L., P. Palazzari, and L. Tarricone, "On the use of numerical phantoms in the study of the human-antenna interaction problem," *IEEE Antennas and Wireless Propagation Letters*, Vol. 2, 43–45, 2003.
22. Catarinucci, L., P. Palazzari, and L. Tarricone, "A parallel variable-mesh FDTD algorithm for the solution of large electromagnetic problems," *Proc. of 19th IEEE International Parallel and Distributed Processing Symposium, IPDPS 2005*, Denver, CO, 2005.
23. Catarinucci, L. and L. Tarricone, "A parallel graded-mesh FDTD algorithm for human-antenna interaction problems," *International Journal of Occupational Safety and Ergonomics*, Vol. 15, No. 1, 45–52, 2009.
24. Zubal, I. G., C. R. Harrell, E. O. Smith, Z. Rattner, G. Gindi, and P. B. Hoffer, "Computerized three-dimensional segmented human anatomy," *Medical Physics*, Vol. 21, No. 2, 299–302, 1994.